

# IKK- $\beta$ -mediated myeloid cell activation exacerbates inflammation and inhibits recovery after spinal cord injury

Junghee Kang<sup>1,2</sup>, Mei Hua Jiang<sup>3</sup>, Hyun Jung Min<sup>1,2</sup>, Eun-Kyeong Jo<sup>4</sup>,  
Soojin Lee<sup>5</sup>, Michael Karin<sup>6</sup>, Tae Young Yune<sup>3</sup> and Sung Joong Lee<sup>1,2</sup>

<sup>1</sup> Department of Neuroscience, School of Dentistry and Dental Research Institute, Brain Korea, Seoul National University, Seoul, Korea

<sup>2</sup> Interdisciplinary Program in Genetic Engineering, Seoul National University, Seoul, Korea

<sup>3</sup> Department of Biochemistry and Molecular Biology, Neurodegeneration Control Research Center and Age-Related and Brain Diseases Research Center, School of Medicine, Kyung Hee University, Seoul, Korea

<sup>4</sup> Department of Microbiology and Infection Signaling Network Research Center, College of Medicine, Chungnam National University, Daejeon, Korea

<sup>5</sup> Department of Microbiology, School of Systems Biology, Chungnam National University, Daejeon, Korea

<sup>6</sup> Laboratory of Gene Regulation and Signal Transduction, School of Medicine, University of California at San Diego, San Diego, CA, USA

Traumatic spinal cord injury (SCI) is followed by massive infiltration and activation of myeloid cells such as neutrophils and macrophages, but the functions of these cells are controversial. In this study, our objective was to elucidate the *in vivo* role of a signaling pathway involved in activation of these innate immune cells in SCI using myeloid cell-specific I $\kappa$ B kinase (IKK)- $\beta$  conditional knockout ( $ikk\beta^{\Delta mye}$ ) mice. In these mice, the  $ikk\beta$  gene has been specifically deleted from myeloid cells, compromising their *in vivo* IKK/NF- $\kappa$ B-dependent activation. We found that  $ikk\beta^{\Delta mye}$  mice had significantly reduced neutrophil and macrophage infiltrations after SCI compared to  $ikk\beta^{+/+}$  controls. SCI-induced proinflammatory gene expression was also reduced in  $ikk\beta^{\Delta mye}$  mice. Reduced neuroinflammation in  $ikk\beta^{\Delta mye}$  mice was accompanied by attenuated neuronal loss and behavioral deficits in motor activity. In addition, the SCI-induced expression of CXC ligand 1 was reduced in  $ikk\beta^{\Delta mye}$  mice, which may be responsible for the reduced neutrophil infiltration in these mice. Our data demonstrate that IKK- $\beta$ -dependent myeloid cell activation potentiates neuroinflammation and neuronal damage after SCI.

**Key words:** CXC ligand 1 (CXCL 1) · I $\kappa$ B kinase- $\beta$  · Macrophage · Neutrophil · Spinal cord injury



Supporting Information available online

## Introduction

Innate immune cells are actively involved in pathogenesis and recovery after spinal cord injury (SCI). In a rat SCI model,

neutrophils infiltrate the primary lesion site within several hours, peak at 12–24 h and disappear after several days [1]. Similarly, blood-derived monocytes/macrophages are detected in and around the lesion 2–3 days after injury and may persist for weeks [2]. Studies on the roles of these immune cells indicate that myeloid cells in the spinal cord produce putative neurotoxic mediators, such as reactive oxygen species (ROS), cytokines and

**Correspondence:** Dr. Sung Joong Lee  
e-mail: sjlee87@snu.ac.kr

proteases, and thereby contribute to secondary damage after SCI [3]. The neurotoxic effects of neutrophils were originally suggested by studies that blocked cell adhesion molecules with antibodies [1, 4]. Administering anti-P-selectin or anti-ICAM-1 antibodies to SCI animal models reduced neutrophil infiltration into the spinal cord and attenuated tissue damage. Similarly, depleting blood monocytes by administering clodronate liposomes improved recovery of functional activity after SCI, indicating that blood-derived macrophages contribute to tissue damage [5].

Activated neutrophils and macrophages, on the other hand, not only express tissue-damaging molecules but also produce neurotrophic and anti-oxidant molecules [6, 7]. In addition, macrophages contribute to neuroregeneration by removing myelin debris, which inhibits neurite outgrowth [8]. Based on these findings, intralésional neutrophil/macrophage infiltration was argued to protect the spinal cord from secondary damage and facilitate recovery after SCI. In support of this model, depletion of blood neutrophils by i.v. administration of anti-Ly6G antibody was found to amplify neurological deficit after SCI [9]. Activated macrophages can also be neuroprotective, as evidenced by a study in which implanting activated macrophages post-injury improved locomotive recovery [10]. Such conflicting reports indicate that the *in vivo* roles of neutrophil/macrophage activation and infiltration in SCI are controversial and far from understood.

In this study, we revisited this question using IKK- $\beta$  kinase (IKK)- $\beta$  conditional knockout mice (*ikk $\beta$  <sup>$\Delta$ mye</sup>*), in which the *ikk $\beta$*  gene has been specifically deleted from myeloid cells, including the majority of neutrophil and macrophage populations [11]. IKK- $\beta$  is a protein kinase responsible for NF- $\kappa$ B activation via various inflammatory stimuli [12]; NF- $\kappa$ B is a key transcription factor responsible for the expressions of inflammatory genes and adhesion molecules [13]. We reasoned that the *ikk $\beta$*  deficiency would interfere with neutrophil/macrophage activation after SCI, allowing for the investigation of the *in vivo* role of IKK- $\beta$ /NF- $\kappa$ B-mediated neutrophil and macrophage activation in SCI.

## Results

### Attenuated myeloid cell infiltration in *ikk $\beta$ <sup>$\Delta$ mye</sup>* mice after SCI

To study the *in vivo* role of IKK- $\beta$ -mediated myeloid cell activation in SCI, we used a well-characterized SCI model, spinal cord hemisection at the T9 level [14] using wild-type (*ikk $\beta$ <sup>+/+</sup>*) and myeloid cell-specific IKK- $\beta$  deficient (*ikk $\beta$  <sup>$\Delta$ mye</sup>*) mice. Neutrophils infiltrated into the injured spinal cord tissue were counted using flow cytometry. Gr-1<sup>+</sup> neutrophils were detected in *ikk $\beta$ <sup>+/+</sup>* mouse spinal cord tissue 6 h post-injury, with numbers further increasing after 24 h (3.0% of total counted cells at 6 h and 5.6% at 24 h) (Fig. 1A and B). In comparison, the neutrophil number in *ikk $\beta$  <sup>$\Delta$ mye</sup>* mouse spinal cord tissue was significantly less, 52 and 59% lower than those in *ikk $\beta$ <sup>+/+</sup>* mice at 6 and 24 h respectively (Fig. 1A and

B). No Gr-1<sup>+</sup> cells were detected in spinal cords of sham-operated mice of either genotype (data not shown). Neutrophil infiltration in *ikk $\beta$  <sup>$\Delta$ mye</sup>* mice was similarly reduced in another SCI model, spinal cord crush injury (Supporting Information Fig. 1A). Macrophages infiltrated the lesion site at a considerably later time point following SCI. By flow cytometry, CD11b<sup>+</sup>/CD45<sup>high</sup> macrophages [15] in the injured spinal cord were found to increase in number to 2.6% at 5 days post-injury (dpi) in *ikk $\beta$ <sup>+/+</sup>* mice

(Fig. 2C and D), and only increased to 1.2% in *ikk $\beta$  <sup>$\Delta$ mye</sup>* mice. The proportion of CD11b<sup>+</sup>/CD45<sup>low</sup> cells, which represent resident microglia [15], did not change significantly after SCI in either *ikk $\beta$ <sup>+/+</sup>* or *ikk $\beta$  <sup>$\Delta$ mye</sup>* mice. It has been reported that macrophages exert different effects on spinal cord injuries depending on their activation type (M1 versus M2) [16]. To characterize the type of tissue-infiltrating macrophages, we immunostained injured spinal cord tissues for iNOS and arginase 1, M1 and M2 macrophage markers, respectively. CD68<sup>+</sup> macrophages in both *ikk $\beta$ <sup>+/+</sup>* and *ikk $\beta$  <sup>$\Delta$ mye</sup>* mice expressed iNOS but not Arginase 1 (Fig. 1E) at 5 dpi, indicating that these macrophages were mostly M1 macrophages. Taken together, these data show that deleting *ikk $\beta$*  from myeloid cells reduced neutrophil/macrophage infiltration into the spinal cord after SCI.

### SCI-induced neutrophil chemoattractants are reduced in *ikk $\beta$ <sup>$\Delta$ mye</sup>* mice

To test whether the reduced neutrophil infiltration in *ikk $\beta$  <sup>$\Delta$ mye</sup>* mice was due to innate characteristics of IKK- $\beta$ -deficient neutrophils, we isolated neutrophils from both *ikk $\beta$ <sup>+/+</sup>* and *ikk $\beta$  <sup>$\Delta$ mye</sup>* mice and assessed the expression of CD11a and CXCR2, an adhesion molecule and a chemokine receptor involved in neutrophil extravasation and migration [17]. CD11a and CXCR2 expression in blood neutrophils from *ikk $\beta$  <sup>$\Delta$ mye</sup>* mice were comparable to *ikk $\beta$ <sup>+/+</sup>* mice both at mRNA and protein levels (Fig. 2A). Similarly, CD11a and CXCR2 expression in tissue-infiltrating neutrophils after SCI were not altered in *ikk $\beta$  <sup>$\Delta$ mye</sup>* mice (Fig. 2B). We also tested the migratory activities of neutrophils from *ikk $\beta$ <sup>+/+</sup>* and *ikk $\beta$  <sup>$\Delta$ mye</sup>* mice by incubating cells in media containing CXC ligand (CXCL) 1, a chemokine specific for neutrophil attraction using Transwell plates (Fig. 2C). Neutrophils from *ikk $\beta$  <sup>$\Delta$ mye</sup>* mice migrated more than cells from *ikk $\beta$ <sup>+/+</sup>* mice (547 ± 15 versus 357 ± 13). These data suggest that the reduced neutrophil infiltration in *ikk $\beta$  <sup>$\Delta$ mye</sup>* mice was not due to an altered migratory capacity of neutrophils in the blood after *ikk $\beta$*  deletion.

We tested whether *ikk $\beta$  <sup>$\Delta$ mye</sup>* mice had altered expression of neutrophil-attracting chemokine in the injured spinal cord (Fig. 2D). At 4 h after SCI, CXCL1 mRNA levels increased by 364-fold in the injured tissue of *ikk $\beta$ <sup>+/+</sup>* mice and declined slightly to 286-fold at 8 h. However, in *ikk $\beta$  <sup>$\Delta$ mye</sup>* mice, CXCL1 mRNA only increased 134-fold at 4 h and 88-fold at 8 h. Similarly, CXCL1 protein expression was reduced in *ikk $\beta$  <sup>$\Delta$ mye</sup>* mice by more than 83% (153 ± 82 versus 26 ± 12) at 1 dpi (Fig. 2E). These data

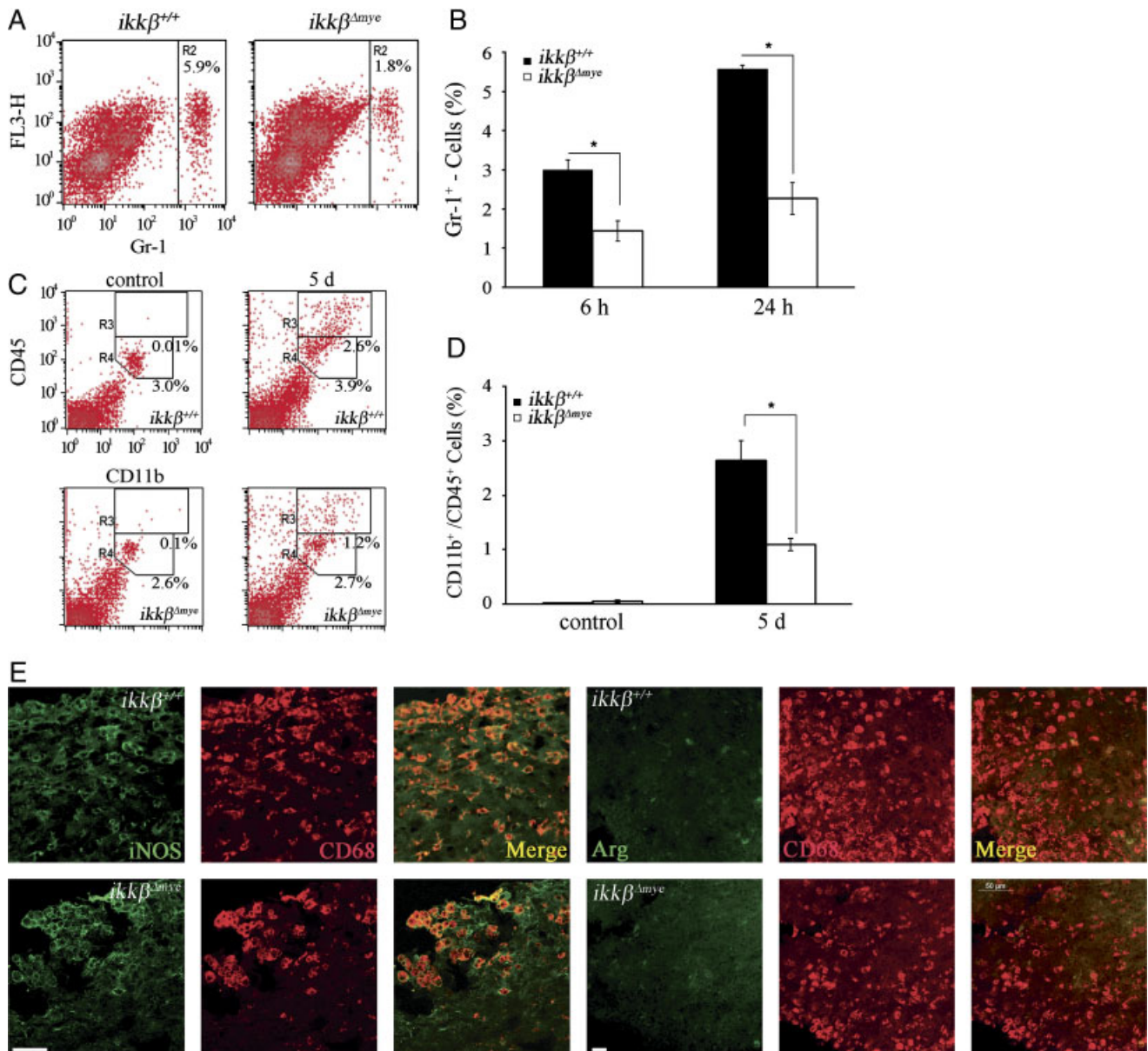


**Figure 1.** Neutrophil and macrophage infiltrations are reduced in *ikkβ<sup>Δmye</sup>* mice. (A) To quantify neutrophils, spinal cord cells were analyzed using flow cytometry with Gr-1 antibody 24 h post-injury. Representative data from three independent experiments with similar results are shown. (B) The graph shows the percentages of Gr-1<sup>+</sup> neutrophils 6 and 24 h post-injury. The data are mean ± SEM of three independent experiments (\**p* < 0.5, one-way ANOVA followed by independent Tukey's post-hoc test). (C and D) CD11b<sup>+</sup>/CD45<sup>high</sup> macrophage population (R3 gate) and CD11b<sup>+</sup>/CD45<sup>low</sup> microglia populations (R4 gate) were analyzed in the injured spinal cords of *ikkβ<sup>+/+</sup>* mice and *ikkβ<sup>Δmye</sup>* mice at 5 dpi using flow cytometry. Representative data from three independent experiments are shown (C), and the mean ± SEM of three independent experiments are shown in a graph (D) (\**p* < 0.5, one-way ANOVA followed by independent Tukey's post-hoc test). (E) CD68<sup>+</sup> (red) macrophages in the injured spinal cord sections of *ikkβ<sup>+/+</sup>* mice and *ikkβ<sup>Δmye</sup>* mice (5 dpi) were co-stained for iNOS (green in left panels) or Arginase 1 (Arg, green in right panels). Representative pictures from three independent experiments are shown. Scale bar, 20 μm. Original magnification, 400 ×.

suggest that reduced expression of neutrophil-attracting chemokines in the injured spinal cord of *ikkβ<sup>Δmye</sup>* mice may, in part, account for low neutrophil infiltration in the lesion site.

CXCL1 is reportedly expressed in spinal cord-infiltrating neutrophils after SCI [18]. We also detected CXCL1 expression in Gr1<sup>+</sup> neutrophils in injured spinal cords (Fig. 2F). To test whether induction of these genes in neutrophils depends on

IKK-β expression, we stimulated neutrophils with LPS, and compared CXCL1 expression in vitro. In neutrophils from *ikkβ<sup>+/+</sup>* mice, LPS stimulation increased CXCL1 transcript levels by 192-fold, whereas the induction was almost completely abrogated in cells from *ikkβ<sup>Δmye</sup>* mice (Fig. 2G). Taken together, these data suggest the possibility that the first neutrophils to arrive at the SCI lesion are less activated in *ikkβ<sup>Δmye</sup>* than in WT

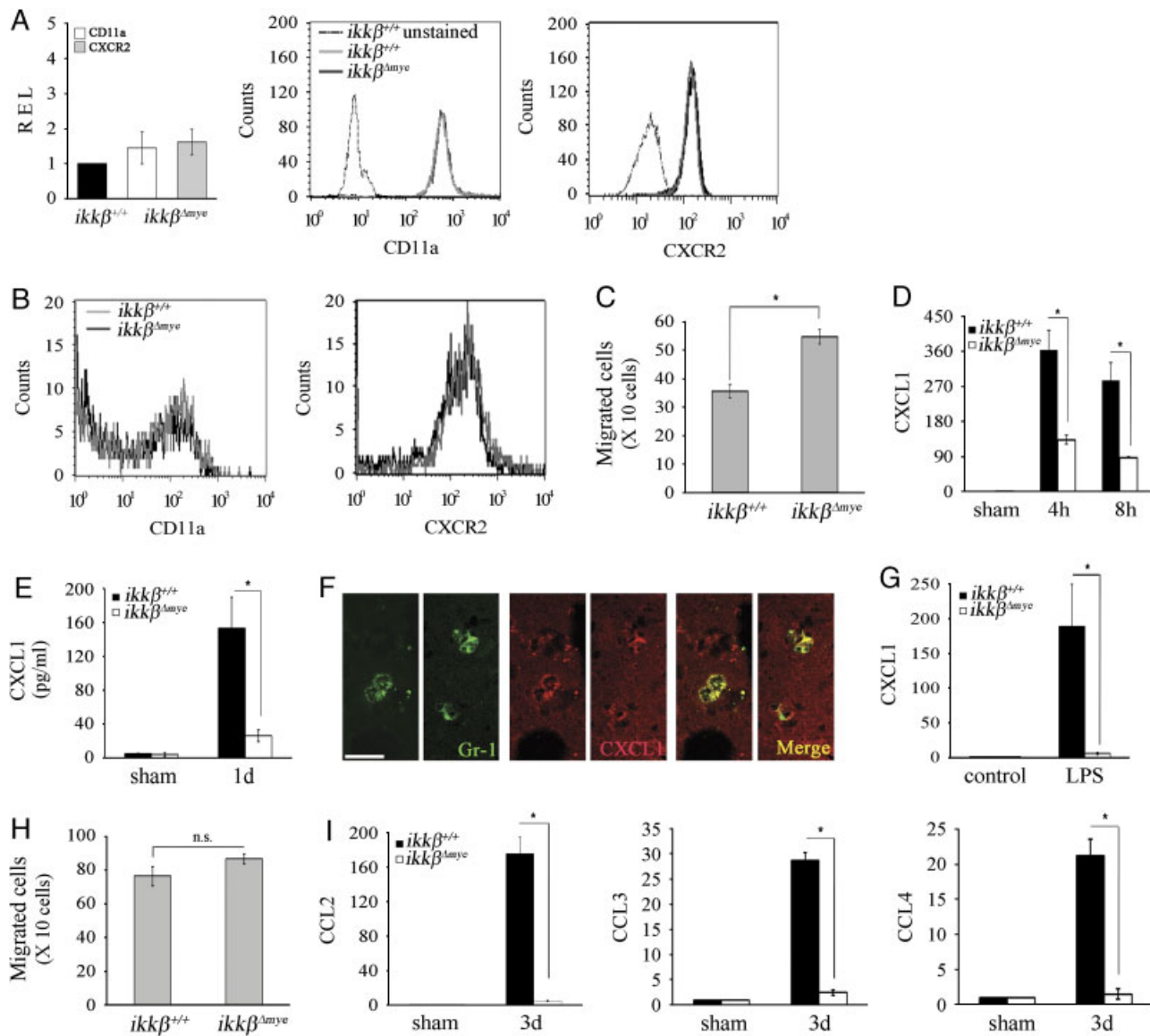


**Figure 2.** SCI-induced neutrophil-attracting chemokine expression is reduced in *ikkβ<sup>Δmye</sup>* mice. (A) Total RNA was prepared from neutrophils isolated from the blood of *ikkβ<sup>+/+</sup>* and *ikkβ<sup>Δmye</sup>* mice blood. CD11a and CXCR2 mRNA levels were measured by real-time RT-PCR (left graph). The relative gene expression levels (REL) in *ikkβ<sup>Δmye</sup>* neutrophils compared to *ikkβ<sup>+/+</sup>* neutrophils are presented ( $n = 3$ ). The data are mean  $\pm$  SEM of three independent experiments. CD11a and CXCR2 levels in *ikkβ<sup>+/+</sup>* and *ikkβ<sup>Δmye</sup>* neutrophils were measured by flow cytometry (right histograms). Representative data from three independent experiments with similar results are shown. (B) CD11a and CXCR2 expressions in Gr-1<sup>+</sup> neutrophils of injured-spinal cord tissue were analyzed by flow cytometry. Representative data from three independent experiments are shown. (C) Neutrophils isolated from *ikkβ<sup>+/+</sup>* and *ikkβ<sup>Δmye</sup>* mice blood were used for migration assays. Neutrophils that migrated into the lower Transwell chamber were counted by light microscopy. (\* $p < 0.05$ , one-way ANOVA followed by independent Tukey's post-hoc test). (D) CXCL1 mRNA level in injured spinal cord of *ikkβ<sup>+/+</sup>* and *ikkβ<sup>Δmye</sup>* mice at 4 and 8 h was assayed using real-time RT-PCR. The data are mean  $\pm$  SEM of three independent experiments (\* $p < 0.05$ , one-way ANOVA followed by independent Tukey's post-hoc test). (E) CXCL1 expression levels in injured spinal cord tissues at 1 dpi were measured by ELISA. The data are mean  $\pm$  SEM of three independent experiments (\* $p < 0.05$ , one-way ANOVA followed by independent Tukey's post-hoc test). (F) To test CXCL1 expression from tissue-infiltrating neutrophils, spinal cord tissue sections of *ikkβ<sup>+/+</sup>* mice at 1 dpi were immunostained with anti-Gr-1 antibody (green) and anti-CXCL1 antibody (red). Representative figures from three independent experiments are shown. Scale bar, 20  $\mu$ m. Original magnification, 630  $\times$ ; scan zoom, 2  $\times$ . (G) Isolated neutrophils from blood were stimulated with LPS (50 ng/mL) for 3 h, and CXCL1 expression was measured by real-time RT-PCR. Means  $\pm$  SEM of three independent experiments are shown (\* $p < 0.05$ , one-way ANOVA followed by independent Tukey's post-hoc test). (H) Monocytes isolated from *ikkβ<sup>+/+</sup>* and *ikkβ<sup>Δmye</sup>* mice were used for migration assays. n.s., not significant. (I) CCL2, 3 and 4 expression in the injured spinal cords of *ikkβ<sup>+/+</sup>* and *ikkβ<sup>Δmye</sup>* mice were measured by real-time RT-PCR. The data are mean  $\pm$  SEM of three independent experiments (\* $p < 0.05$ , one-way ANOVA followed by independent Tukey's post-hoc test).

mice, resulting in reduced chemokine expression. This might further attenuate neutrophil recruitment to the lesion at later time points.

We also assessed monocyte migration in *ikkβ<sup>+/+</sup>* and *ikkβ<sup>Δmye</sup>* mice. Migration of *ikkβ<sup>Δmye</sup>* monocytes stimulated by CCL2 was not significantly different from *ikkβ<sup>+/+</sup>* monocytes

(Fig. 2H). Expression of CD11b or CD11c, adhesion molecules preferentially expressed on myeloid cells, was not significantly different in  $ikk\beta^{+/+}$  or  $ikk\beta^{\Delta mye}$  blood leukocytes (Supporting Information Fig. 2). However, CCL2, 3 and 4 expression in the injured spinal cord was almost completely blocked in  $ikk\beta^{\Delta mye}$  mice (Fig. 2I). These data once again suggest that reduced myeloid cell infiltration in  $ikk\beta^{\Delta mye}$  mice is not due to reduced migratory activity of the IKK- $\beta$ -deficient cells but is more likely due to the reduced expression of chemoattractants in lesions of the  $ikk\beta^{\Delta mye}$  mice.

### Compromise of SCI-induced neuronal cell death and behavioral deficit in $ikk\beta^{\Delta mye}$ mice

To address the effects of myeloid cell activation and infiltration on SCI, we measured lesion volume in the spinal cords of  $ikk\beta^{+/+}$  and  $ikk\beta^{\Delta mye}$  mice after hemisection injury (Fig. 3A). The lesion volume in  $ikk\beta^{\Delta mye}$  mice spinal cord was 30% less than the volume in  $ikk\beta^{+/+}$  mice at 28 dpi. We then examined neurons in the coronal and longitudinal sections of injured spinal cords by immunohistochemistry using anti-NeuN antibody. Five days after

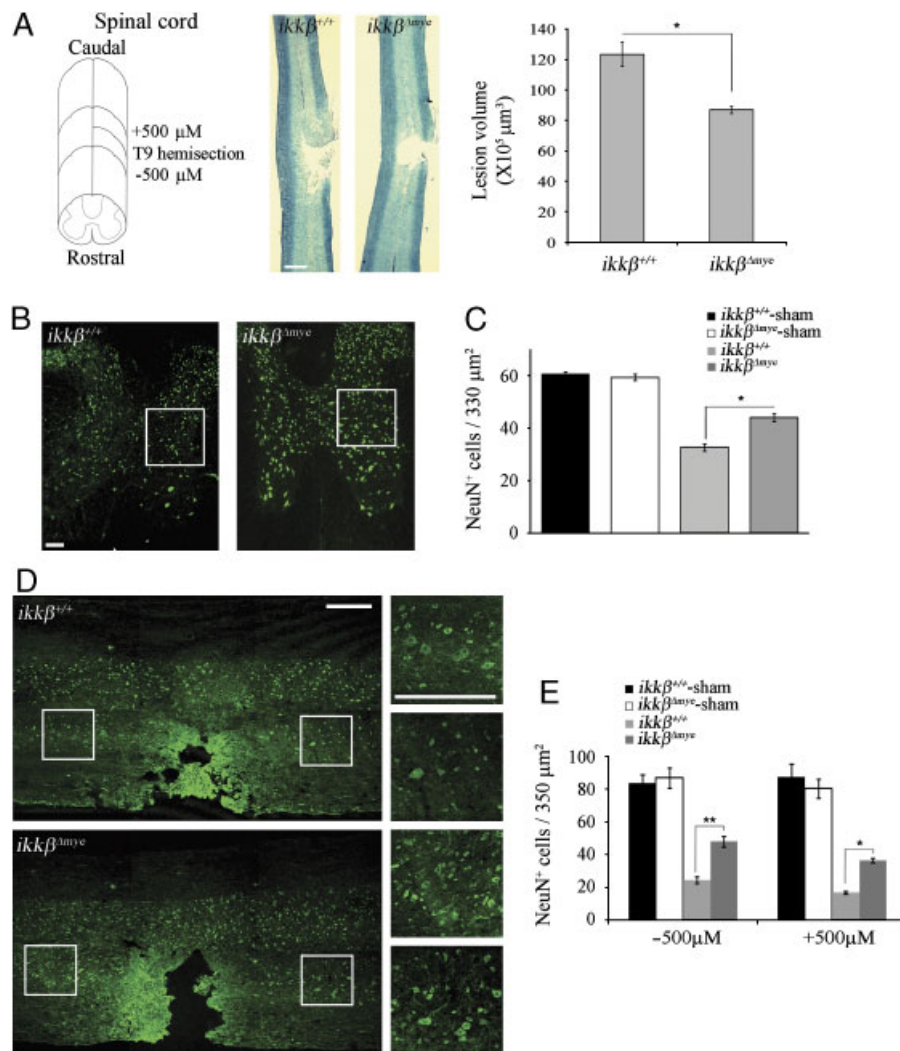


**Figure 3.** SCI-induced neuronal cell death is attenuated in  $ikk\beta^{\Delta mye}$  mice. (A) At 28 dpi, coronal and longitudinal sections were prepared from tissue within 500  $\mu\text{m}$  of the lesion in SCI-induced or sham-operated mice. Spinal cord sections were stained with luxol fast blue. Scale bar, 500  $\mu\text{m}$ . Total lesion volume was calculated from 68 sections per animal ( $n = 3$ ,  $*p < 0.5$ , one-way ANOVA followed by independent Tukey's post-hoc test). (B) Neurons in coronal sections of  $ikk\beta^{\Delta mye}$  mice and  $ikk\beta^{+/+}$  mice were detected by immunohistochemistry using anti-NeuN antibodies. Scale bar, 100  $\mu\text{m}$ . Original magnification, 100 $\times$ . A representative picture of a coronal section at  $-500 \mu\text{m}$  in the ipsilateral region is shown. (C) NeuN<sup>+</sup> cells in the 330  $\mu\text{m}^2$  white rectangle area (ipsi-region)  $-500 \mu\text{m}$  from the lesion site in the spinal cord of sham-operated  $ikk\beta^{+/+}$  mice ( $ikk\beta^{+/+}$ -sham), sham-operated  $ikk\beta^{\Delta mye}$  mice ( $ikk\beta^{\Delta mye}$ -sham), SCI-injured  $ikk\beta^{+/+}$  mice ( $ikk\beta^{+/+}$ ) and SCI-injured  $ikk\beta^{\Delta mye}$  mice ( $ikk\beta^{\Delta mye}$ ) were quantified. Six slides from three animals were counted, and the means  $\pm$  SEM are presented ( $*p < 0.5$ , one-way ANOVA followed by independent Tukey's post-hoc test). (D) Neurons in the spinal cord longitudinal sections were detected by immunohistochemistry using anti-NeuN antibody. Scale bar, 100  $\mu\text{m}$ . Original magnification, 100 $\times$ . A representative image is shown. (E) NeuN<sup>+</sup> cells in the 350  $\mu\text{m}^2$  white rectangle area  $\pm 500 \mu\text{m}$  from the lesion site in the spinal cord of  $ikk\beta^{+/+}$ -sham,  $ikk\beta^{\Delta mye}$ -sham,  $ikk\beta^{+/+}$  and  $ikk\beta^{\Delta mye}$  mice were quantified. Eight slides from four animals were counted, and the means  $\pm$  SEM are presented ( $*p < 0.005$ ,  $**p < 0.05$ , one-way ANOVA followed by independent Tukey's post-hoc test).

SCI, there were 46% fewer NeuN<sup>+</sup> neurons in the region ipsilateral to the lesion site in *ikkβ*<sup>+/+</sup> mice than in sham-operated mice (Fig. 3C). However, in *ikkβ*<sup>Δmye</sup> mice, more NeuN<sup>+</sup> neurons were detected in the injured spinal cord (Fig. 3B). In *ikkβ*<sup>Δmye</sup> mice, there were 33% more NeuN<sup>+</sup> neurons per unit area rostral (−500 μm) to the lesion site than in *ikkβ*<sup>+/+</sup> mice (33 versus 44) (Fig. 3C). Similarly, we found an increase in NeuN<sup>+</sup> cells in the longitudinal sections (±500 μm to the lesion site) of injured spinal cords in *ikkβ*<sup>Δmye</sup> mice (Fig. 3D). Compared to *ikkβ*<sup>Δmye</sup> mice, the number of NeuN<sup>+</sup> neurons in *ikkβ*<sup>+/+</sup> mice was 54% (25 versus 48) at the rostral site and 49% (17 versus 37) at the caudal site (Fig. 3E). Neuronal cell death in *ikkβ*<sup>Δmye</sup> mice was also compromised after spinal cord crush injury (Supporting Information Fig. 1B). These data demonstrate that IKK-β-mediated myeloid cell activation and infiltration in injured spinal cords contribute to neuronal cell death after SCI.

To characterize the nature of cell death after SCI, we measured apoptotic cells in the lesion area by terminal deoxynucleotidyl transferase dUTP nick end labeling (TUNEL) staining (Fig. 4A). One day after SCI, TUNEL-positive apoptotic cells were detected close to the lesion site in *ikkβ*<sup>+/+</sup> mice, co-

localizing with NeuN<sup>+</sup> neurons (Fig. 4A, white arrows), shown magnified in Fig. 4B. In addition, active caspase-3 expression colocalized to NeuN<sup>+</sup> neurons at 24 h post-injury (Fig. 4D, white arrows). Thus, neurons in the lesion underwent apoptosis 1 day after spinal hemisection injury in *ikkβ*<sup>+/+</sup> mice. In *ikkβ*<sup>Δmye</sup> mice, however, few TUNEL<sup>+</sup> or caspase-3<sup>+</sup> neurons were detected at the lesion (Fig. 4A, lower panels, and D, right panel, and 4C). Since we did not detect any obvious macrophage infiltration into the lesion site within 24 h of injury, IKK-β-mediated neutrophil activation was likely involved in neuronal apoptosis at 1 dpi. This might eventually have resulted in the reduced number of neurons in *ikkβ*<sup>+/+</sup> mice compared to *ikkβ*<sup>Δmye</sup> mice at the later time point.

To test whether the reduced cell death in *ikkβ*<sup>Δmye</sup> mice affects functional recovery from SCI, we determined the Basso Mouse Scale (BMS) scores [19] of injured mice (Fig. 5). Up to 3 days after injury, no difference in motor function was observed between *ikkβ*<sup>+/+</sup> and *ikkβ*<sup>Δmye</sup> mice. After 7 days, the average BMS score of *ikkβ*<sup>Δmye</sup> mice was higher than *ikkβ*<sup>+/+</sup> mice, showing that lack of myeloid IKK-β improved recovery after SCI.

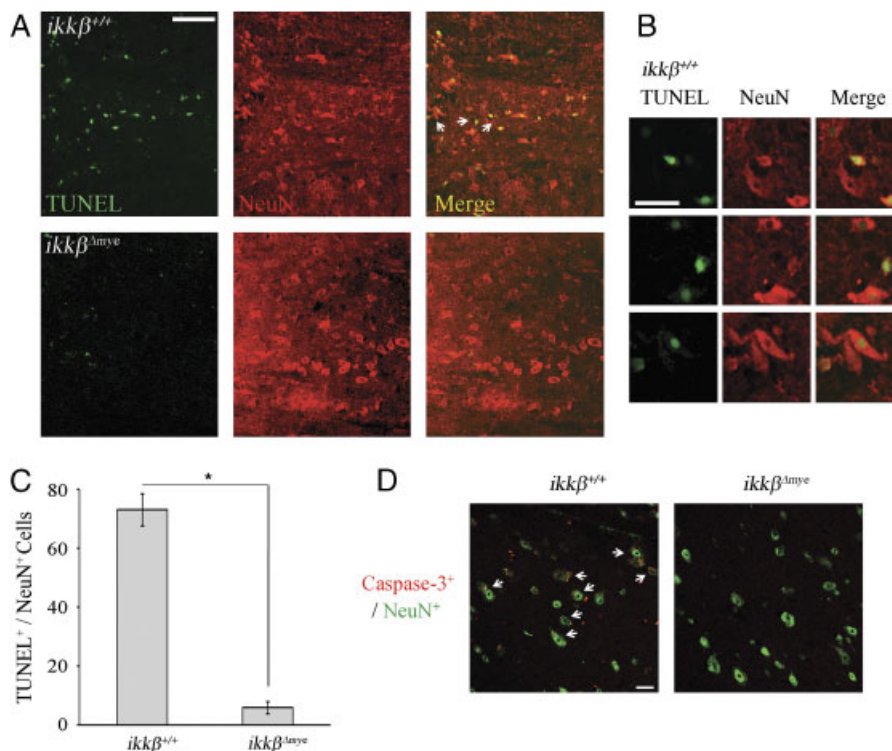


**Figure 4.** Apoptotic neuronal cell death is reduced in *ikkβ*<sup>Δmye</sup> mice. (A) Spinal cord sections prepared 1 dpi were used for TUNEL (green) staining, and the same sections were used for anti-NeuN (red) immunostaining. DNA fragmentation in neurons was detected at the lesion boundary of *ikkβ*<sup>+/+</sup> mice. Scale bar, 50 μm. Arrows indicate areas that are magnified in (B). Original magnification, 200 ×. A representative figure from three independent experiments with similar results is shown. (B) Magnified images indicated by arrows in (A) Scale bar, 20 μm. (C) All TUNEL<sup>+</sup> and NeuN<sup>+</sup> cells in each section were counted and shown in a graph. Means ± SEM of three independent experiments are shown (\**p*<0.005, one-way ANOVA followed by independent Tukey's post-hoc test). (D) Spinal cord sections prepared 1 dpi were immunostained for active caspase-3 (red) and NeuN<sup>+</sup> (green). Immunoreactivity of active caspase-3 was detected in NeuN<sup>+</sup> cells in the sections of *ikkβ*<sup>+/+</sup> mice (arrows). Representative figure from three independent experiments with similar results is shown. Scale bar, 20 μm. Original magnification, 400 ×.

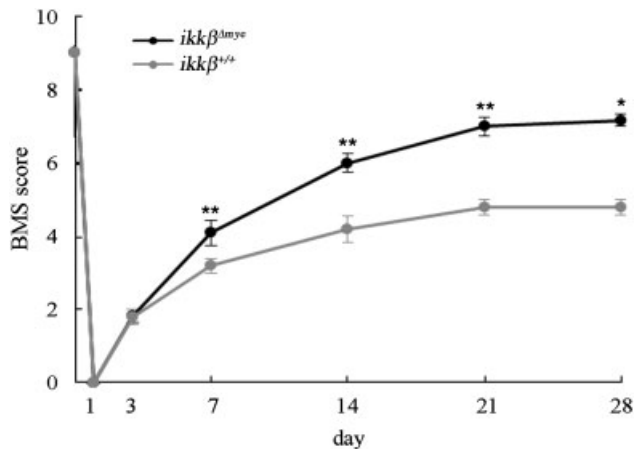


**Figure 5.** Improved functional recovery after SCI in *ikkβ<sup>Δmye</sup>* mice. BMS tests were carried out in an open field over 28 days after SCI in *ikkβ<sup>+/+</sup>* ( $n = 5$ ) and *ikkβ<sup>Δmye</sup>* mice ( $n = 6$ ) (\* $p < 0.05$ , \*\* $p < 0.05$ , two-way ANOVA followed by Tukey's post-hoc test).

### Reduced ROS and reactive nitrogen species production after SCI in *ikkβ<sup>Δmye</sup>* mice

To identify the mechanisms underlying differences in the rates of neuronal apoptosis, we measured neurotoxic gene expression in injured spinal cord tissue. Previous studies suggest that neuronal cell death is induced by proinflammatory cytokines and ROS generated by neutrophils [20, 21]. Therefore, we measured the mRNA expression of IL-6, IL-1 $\beta$  and TNF- $\alpha$  in injured spinal cords of *ikkβ<sup>+/+</sup>* and *ikkβ<sup>Δmye</sup>* mice. Four hours after injury, when neutrophils begin to infiltrate the injured tissue, IL-6, IL-1 $\beta$  and TNF- $\alpha$  mRNAs increased by 85-, 160- and 21-fold, respectively, in *ikkβ<sup>+/+</sup>* mice (Fig. 6A). However, in *ikkβ<sup>Δmye</sup>* mice, the mRNA levels increased by only 18-, 43- and 3-fold respectively. Similarly, induction of iNOS, which is involved in reactive nitrogen species production, and COX-2, which is involved in ROS generation, were attenuated in *ikkβ<sup>Δmye</sup>* mice compared to *ikkβ<sup>+/+</sup>* (two-fold versus five-fold for iNOS expression at 8 h; four-fold versus 13-fold for COX-2 expression at 4 h) (Fig. 6B and C). Nitric oxide (NO) and superoxides generated by iNOS and COX-2 may cause neuronal cell death via nitrotyrosylation and DNA damage [22, 23]. To examine whether protein nitrotyrosylation and DNA damage were involved in SCI-induced neuronal death, we measured the levels of nitrotyrosylated proteins and 8-hydroxy-guanine (8-OHG) incorporation into DNA in the spinal cord by immunostaining. After injury, nitrotyrosine and 8-OHG-immunoreactive cells were detected in the lesion areas of *ikkβ<sup>+/+</sup>* mice (Fig. 6D and E). The number of immunoreactive cells was much lower in *ikkβ<sup>Δmye</sup>* mice (Fig. 6D and E). NO activates neuronal matrix metalloproteinase-9 (MMP-9) through nitrotyrosylation, leading to neuronal apoptosis [24]. To test if SCI-induced NO production and subsequent tyrosine nitrotyrosylation leads to neuronal MMP-9 activation, we measured the MMP-9 activity in the injured spinal cord by in situ zymography (Fig. 7A). In *ikkβ<sup>+/+</sup>* mice,

gelatinolytic activity was detected in many cells near the lesion site, which mostly co-localized with NeuN<sup>+</sup> neurons, but not with Gr-1<sup>+</sup> neutrophils (Fig. 7A and B). However, the injured spinal cord of *ikkβ<sup>Δmye</sup>* mice showed markedly reduced gelatinase-active neuronal cells (Fig. 7A, lower panels). We also measured MMP-9 mRNA in the spinal cord. MMP-9 transcripts were upregulated by ten-fold at 8 h post-injury in *ikkβ<sup>+/+</sup>* spinal cords, with little or no induction in *ikkβ<sup>Δmye</sup>* mice (Fig. 7C). These data show that increased MMP-9 expression in injured *ikkβ<sup>+/+</sup>* mice might contribute to the enhanced MMP-9 activity observed in these mice. Taken together, these data imply that, in *ikkβ<sup>Δmye</sup>* mice, reduced reactive nitrogen species and ROS production and MMP-9 activation might, at least in part, account for the reduced neuronal apoptosis after SCI in these mice.

## Discussion

In this study, we tested the in vivo role of IKK- $\beta$  activation in neutrophils responding to SCI. Previously, conflicting results suggested both beneficial and detrimental roles of neutrophil activation and infiltration after SCI. Our results showing that ablating IKK- $\beta$  reduced morphological and behavioral deficits after SCI are consistent with previous studies that suggest a detrimental role for neutrophils in SCI secondary damage. Our study is distinct from a recent study that used a Ly6G/Gr-1 antibody to deplete blood neutrophils [9]. In that study, Gr-1<sup>+</sup> cells consisting of mainly, but not exclusively, neutrophils were depleted from the circulatory system. In contrast, *ikkβ<sup>Δmye</sup>* mice did not lose blood neutrophils (data not shown), and only IKK/NF- $\kappa$ B-mediated responses were compromised. Although it is speculative, neutrophils in a resting state might possibly have a neuroprotective role, so depleting the total neutrophil population worsens the neurological outcome after SCI.

In *ikkβ<sup>Δmye</sup>* mice, the IKK- $\beta$  gene was deleted not only in neutrophils but also in a majority of monocytes/macrophages. Therefore, the phenotype observed in these mice cannot be attributed solely to IKK- $\beta$  deficiency in neutrophils. In our study, however, leukocytes infiltrating the lesion at early time points were mostly neutrophils, and we did not detect any macrophage infiltration within 24 h post-injury. Neuronal apoptosis was clear at 24 h post-injury in *ikkβ<sup>+/+</sup>* but not *ikkβ<sup>Δmye</sup>* mice. These findings argue that the early effects on neuronal apoptosis were most likely due to neutrophil activation and infiltration, not macrophages. Therefore, we deduced that IKK- $\beta$ -dependent neutrophil activation contributed to neuronal damage at early time points. In *ikkβ<sup>Δmye</sup>* mice, macrophage infiltration was also reduced at later time points. It has been reported that macrophage infiltration impedes functional recovery after SCI [5]. Therefore, the relative improvement in behavioral recovery observed in *ikkβ<sup>Δmye</sup>* mice cannot be totally attributed to inhibiting neutrophil activation and infiltration. Rather, it might be the result of combined neutrophil and macrophage activation. Thus far, we have not been able to dissect the relative contributions of each cell type to behavioral deficits. Of note, an

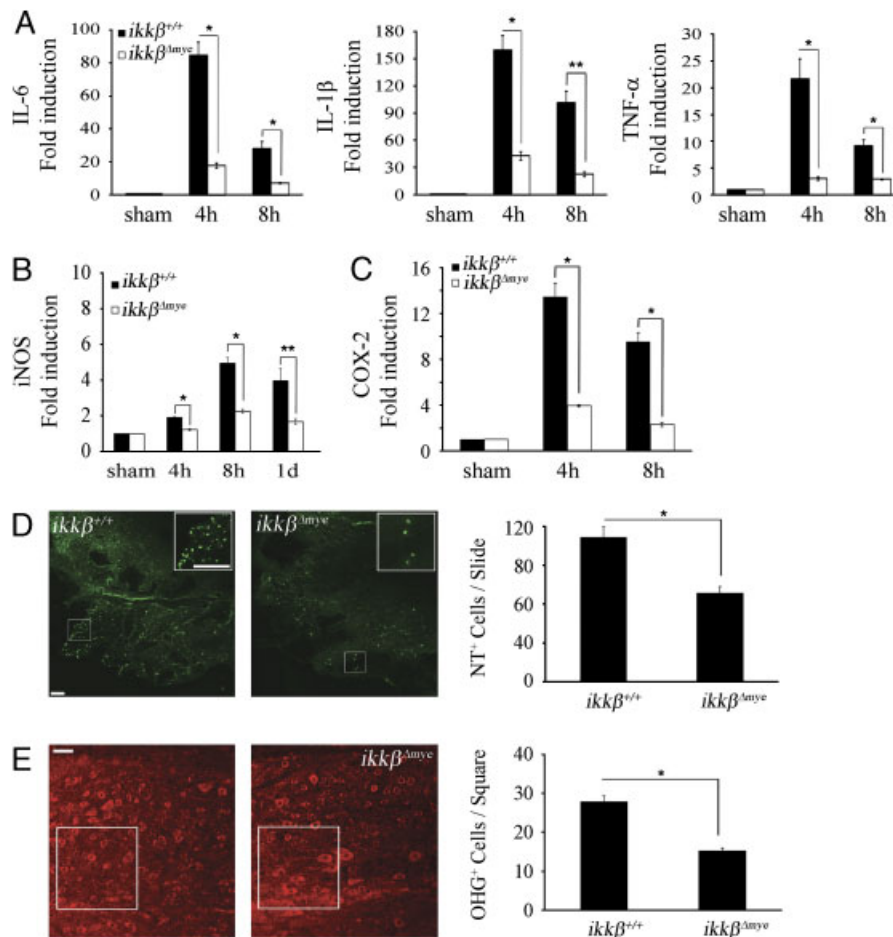


**Figure 6.** Expression of SCI-induced proinflammatory cytokines, iNOS and COX-2 are attenuated in *ikkβ<sup>Δmye</sup>* mice. (A) Spinal cords of sham-operated and SCI-injured *ikkβ<sup>+/+</sup>* and *ikkβ<sup>Δmye</sup>* mice were isolated 4 and 8 h post-injury. Real-time RT-PCR was used to measure IL-6, IL-1β and TNF-α levels. Means ± SEM of three independent experiments are shown (\* $p < 0.05$ , \*\* $p < 0.05$ , one-way ANOVA followed by independent Tukey's post-hoc test). mRNA levels of iNOS (B) and COX-2 (C) in the spinal cord at different time points after SCI, as measured by real-time RT-PCR (\* $p < 0.05$ , \*\* $p < 0.05$ , one-way ANOVA followed by independent Tukey's post-hoc test). (D) Tyrosine nitrosylated-proteins in the injured spinal cords of *ikkβ<sup>+/+</sup>* and *ikkβ<sup>Δmye</sup>* mice were detected by immunostaining using anti-nitrotyrosine antibodies. Nitrotyrosine immunoreactivity was detected as particulates in the cells surrounding the lesion site at 1 dpi in *ikkβ<sup>+/+</sup>* mice. Representative figure from three independent experiments with similar results is shown. Scale bar, 20 μm. Original magnification, 100 ×. NT<sup>+</sup> cells in each section were counted and are shown in a graph. Means ± SEM of three independent experiments are shown (\* $p < 0.05$ , one-way ANOVA followed by Tukey's post-hoc test). (E) ROS-damaged cells in the injured spinal cord were detected by immunostaining with anti-8-OHG antibodies. Representative figure from three independent experiments with similar results is shown. Scale bar, 50 μm. Original magnification, 200 ×. OHG<sup>+</sup> cells in the white square area (40 000 μm<sup>2</sup>) 150 μm caudal from the spinal cord lesion site were quantified. Six slides from three animals were counted, and the means ± SEM are presented (\* $p < 0.05$ , one-way ANOVA followed by Tukey's post-hoc test).

approximately 50% reduction in neuronal cell number was observed in the injured spinal cords of *ikkβ<sup>Δmye</sup>* mice compared to sham-operated mice, as measured by NeuN-immunostaining, but very few TUNEL-positive cells were detected in *ikkβ<sup>Δmye</sup>* mice at 1 dpi. These data imply that neuronal cells also underwent non-apoptotic cell death in these mice, and this cell death was not greatly affected by neutrophil infiltration and activation.

To elucidate the molecular mechanisms underlying the reduced neutrophil and macrophage infiltrations in *ikkβ<sup>Δmye</sup>* mice, we tested the innate migratory activities of neutrophils and monocytes from *ikkβ<sup>Δmye</sup>* mice. Our data showed that IKK-β deficiency did not alter the migratory activities of these cells. Therefore, neutrophil- and macrophage-recruitment are more

likely impaired in *ikkβ<sup>Δmye</sup>* mice due to defective production of neutrophil- and macrophage-attracting chemokines after SCI. Indeed we found that SCI-induced CXCL1 expression is severely compromised in *ikkβ<sup>Δmye</sup>* mice and LPS-mediated CXCL1 expression in vitro was eliminated in *ikkβ<sup>Δmye</sup>* neutrophils. Based on these data, we speculated that neutrophils that initially infiltrated the spinal cord of injured *ikkβ<sup>Δmye</sup>* mice did not express CXCL1, so they did not further augment neutrophil infiltration. This might explain the observed differences in the post-SCI neutrophil infiltration rate between *ikkβ<sup>+/+</sup>* and *ikkβ<sup>Δmye</sup>* mice.

We also found that the expression levels of proinflammatory cytokines (IL-1β, IL-6 and TNF-α), iNOS, COX-2 and MMP-9 were

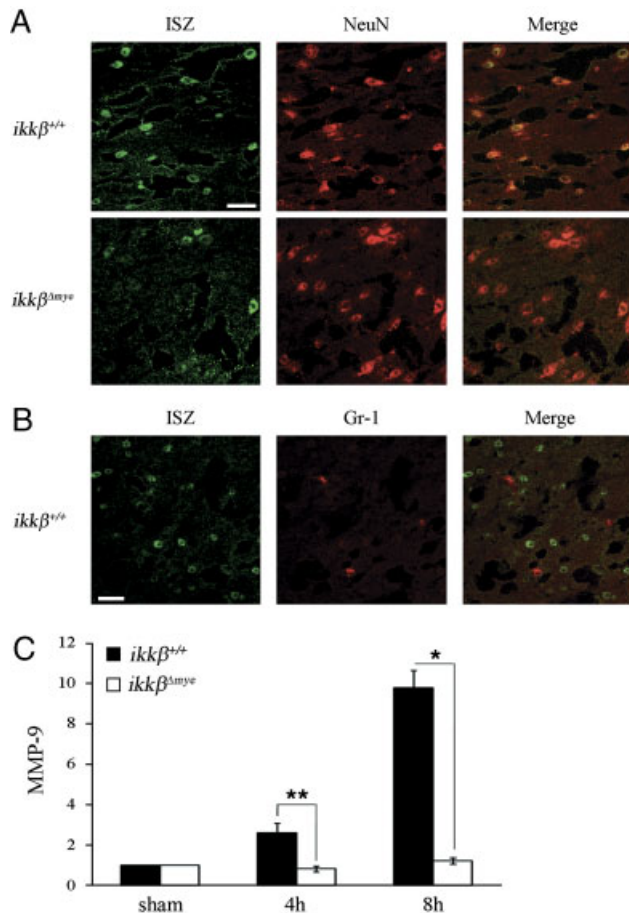


**Figure 7.** Localization of gelatinolytic activity in neurons and MMP expression after SCI. (A) Cryostat tissue sections at 6 h post-SCI were used for in situ zymography (ISZ) and NeuN immunostaining and number of cells with gelatinolytic activity was measured in *ikkβ<sup>Δmye</sup>* mice (lower panels) and *ikkβ<sup>+/+</sup>* mice (upper panels). Representative figure from three independent experiments with similar results is shown. Scale bar, 20 μm. Original magnification, 400×. Gelatinolytic activity co-localized with NeuN<sup>+</sup> neurons (A) but not Gr-1<sup>+</sup> neutrophils (B). (C) Real-time RT-PCR of MMP-9 from injured spinal cord tissue of *ikkβ<sup>+/+</sup>* and *ikkβ<sup>Δmye</sup>* mice at 4 and 8 h after injury. The data are means ± SEM of three independent experiments (\**p* < 0.05, \*\**p* < 0.05, one-way ANOVA followed by independent Tukey's post-hoc test).

lower in injured spinal cords of *ikkβ<sup>Δmye</sup>* mice than in WT mice. All of these proinflammatory cytokines are implicated in neuronal apoptosis [25]. NO and prostaglandin E (PGE), which are produced by iNOS and COX-2, respectively, induce neuronal apoptosis by nitrotyrosylation of proteins or DNA damage [23, 26]. We found reduced nitrotyrosylation and DNA damage in the injured spinal cords of *ikkβ<sup>Δmye</sup>* mice compared to *ikkβ<sup>+/+</sup>* mice. In addition, neuronal gelatinase activation was attenuated in *ikkβ<sup>Δmye</sup>* mice, probably because of the combined effects of reduced MMP-9 expression and MMP-9 nitrotyrosylation. MMP-9 activation is a key event in neuronal apoptosis [27], although the underlying molecular mechanisms are not completely understood. Our data imply that reduced proin-

flammatory cytokines, NO and prostaglandin E in *ikkβ<sup>Δmye</sup>* mice might contribute to reduced neuronal apoptosis at 24 h post-injury. Again, since IKK-β is deficient only in neutrophils and macrophages, and only neutrophils infiltrate at 24 h post-injury, the differences in the above genes are likely in neutrophils. This is supported by in vitro studies using neutrophils cultured from *ikkβ<sup>+/+</sup>* and *ikkβ<sup>Δmye</sup>* mice. Of note, we found that LPS-induced inflammatory gene expression was completely blocked in *ikkβ<sup>Δmye</sup>* neutrophils, although expression of these genes was only partially reduced in vivo. This implies that cells other than the tissue-infiltrating neutrophils express these genes in the spinal cord after SCI, although we did not demonstrate this experimentally.

In conclusion, the results of our study demonstrate that IKK-β-dependent neutrophil activation and infiltration in the injured spinal cord potentiated inflammation and neuronal damage and impeded functional recovery after SCI.

## Materials and methods

### Mice and SCI

Myeloid cell type-specific IKK-β-deficient (*ikkβ<sup>Δmye</sup>*) mice were generated by crossing floxed-*ikkβ* (*ikkβ<sup>F/F</sup>*) mice and LysM-Cre knock-in mice expressing Cre under the control of the endogenous lysozyme M promoter, as described previously [28, 29]. Both mouse lines were of C57BL/6 background. Adult male mice (8–10 wk old) were anesthetized with sodium pentobarbital (30 mg/kg body weight, i.p.) and laminectomized between T8 and T10. The exposed spinal cord was subjected to lateral hemisection at the T9 level with mini-Vannas scissors under microscope visualization.

All surgical and experimental procedures were reviewed and approved by the Institutional Animal Care and Use Committee (IACUC) at Seoul National University.

**Table 1.** Primary antibodies used for immunohistochemistry

Antibody	Titer	Company
Mouse anti-NeuN	1:1000	Chemicon
Rat anti-CD68	1:500	Serotec (Oxford, UK)
Rat anti-Gr-1	1:1000	Invitrogen (Carlsbad, CA, USA)
Rabbit anti-caspase-3	1:200	Santa Cruz Biotechnology (Santa Cruz, CA, USA)
Mouse anti-iNOS	1:100	Santa Cruz Biotechnology
Rabbit anti-arginase I	1:100	Santa Cruz Biotechnology
Goat anti-CXCL1	1:10	R&D Systems (Minneapolis, MN, USA)
Rabbit anti-nitrotyrosine	1:500	Upstate (Temecula, CA, USA)
Mouse anti-8-hydroxyguanosine	1:1000	Abcam (Cambridge, MA, USA)

## Immunohistochemistry

Immunohistochemistry was performed as previously described [30]. Information on the antibodies used in this study is provided in Table 1.

## Luxol fast blue staining and lesion volume measurement

Luxol fast blue staining was performed to calculate lesion volume as previously described [31]. Images of the stained sections were taken under microscope (Axiovert200, Carl Zeiss, Munchen, Germany) and the lesion size (x–y stage) was calculated using the Axiovision 4.8 image program. The total lesion volume was calculated by summing individual subvolumes following the Cavalieri method [32].

## TUNEL staining

Apoptotic cells were detected using an Apoptaq Plus Fluorescein in situ cell apoptosis detection kit (Chemicon, Temecula, CA, USA) according to the manufacturer's instructions.

## Real-time RT-PCR

Real-time RT-PCR was performed as previously described [33]. Relative mRNA levels were calculated according to the  $2^{-\Delta\Delta Ct}$  method [34]. All Ct values were normalized to GAPDH. All experiments were performed at least three times. The PCR primer sequences used in this study are listed in Table 2.

## Behavioral tests

Hind limb motor function was assessed by open field locomotion using BMS [19]. All behavioral tests were performed blind.

## Neutrophil and monocyte isolation and migration assay

Neutrophils and monocytes were prepared as described previously [35, 36]. Isolated neutrophil or monocyte cells ( $5 \times 10^4$  cells/well) were seeded onto a 5- $\mu$ m pore-size Transwell plate (Costar, Corning, NY, USA) and incubated for 2 h in culture medium, in the presence or absence of CXCL1 (100 ng/mL, Bio-Research Products, South Lancaster, MA, USA) or CCL2 (50 ng/mL, Bio-Research Products) in the lower chamber. Neutrophils or monocytes that had migrated into the lower chamber were counted under magnification.

## In situ zymography

In situ gelatinolytic activity was detected as described previously [37].

## Flow cytometry

Flow cytometry was performed as previously described [30]. PE-conjugated anti-CD11a (eBioscience, San Diego, CA, USA), FITC-conjugated anti-CD11b (BD Pharmingen, San Diego, CA, USA), PE-conjugated anti-CD45 (BD Pharmingen), FITC-conjugated anti-Gr-1 (BioLegend, San Diego, CA, USA) or Cy5.5-conjugated anti-CXCR2 (BioLegend) antibodies were used for flow cytometry.

## ELISA

Spinal cord tissues ( $\pm 0.25$  cm to the injury site) were dissected from the spinal cord and proteins were extracted using tissue lysis buffer (137 mM NaCl, 20 mM Tris-HCl, 1% NP40, and protease inhibitor cocktail set III (Calbiochem, La Jolla, CA, USA)). The KC/CXCL1 in the tissue lysates was measured using ELISA kit

**Table 2.** Primer sequences used for real-time RT-PCR

Gene	Forward primer	Reverse primer	GenBank no.
Mouse GAPDH	5'-AGG TCA TCC CAG AGC TGA ACG-3'	5'-CAC CCT GTT GCT GTA GCC GTA T-3'	NM_008084
Mouse IL-6	5'-GCC CTT CAG GAA CAG CTA TG-3'	5'-CAG AAT TGC CAT TGC ACA AC-3'	NM_012589
Mouse IL-1 $\beta$	5'-TTG TGG CTG TGG AGA AGC TGT-3'	5'-AAC GTC ACA CAC CAG CAG GTT-3'	NM_008361
Mouse TNF- $\alpha$	5'-AGC AAA CCA CCA AGT GGA GGA-3'	5'-GCT GGC ACC ACT AGT TGG TTG T-3'	NM_013693
Mouse iNOS	5'-TCT GTG CCT TTG CTC ATG ACA-3'	5'-TGC TTC GAA CAT CGA ACG TC-3'	NM_012611
Mouse COX-2	5'-CAG TAT CAG AAC CGC ATT GCC-3'	5'-GAG CAA GTC CGT GTT CAA GGA-3'	U03389
Mouse CXCL1	5'-CCG AAG TCA TAG CCA CAC TCA A-3'	5'-GCA GTC TGT CTT CTT TCT CCG TTA C-3'	NM_008176
Mouse CXCR2	5'-GGT GGG GAG TTC GTG TAG AA-3	5'-CGA GGT GCT AGG ATT TGA GC-3	BC051677.1
Mouse CD11a	5'-AGA TCG AGT CCG GAC CCA CAG-3'	5'-GGC AGT GAT AGA GGC CTC-3'	NM_008400.2
Mouse CCL2	5'-TCA GCC AGA TGC AGT TAA CG-3'	5'-GAT CCT CTT GTA GCT CTC CAG C-3'	BC05507
Mouse CCL3	5'-ACT GCC TGC TGC TTC TCC TAG A-3'	5'-AGG AAA ATG ACA CCT GGC TGG-3'	BC111443
Mouse CCL4	5'-TCC CAC TTC CTG CTG TTT CTC T-3'	5'-GAA TAC CAC AGC TGG CTT GGA-3'	NM_013652.2
Mouse MMP-9	5'-TGT ACG GAC CCG AAG C-3'	5'-CCG TCC TTA TCG TAG TCA G-3'	NM_013599

(R&D Systems, Minneapolis, MN, USA) according to the manufacturer's instructions.

### Statistical analysis

Data are presented as mean  $\pm$  SEM. Statistical analyses for real-time PCR data, flow cytometry data, cell migration assay data, ELISA data and image analysis were performed using a one-way ANOVA for measurements, followed by an independent Tukey's post-hoc test to compare the procedures. A  $p < 0.5$  was considered statistically significant. Statistical analysis for motor behavioral tests was performed using two-way ANOVA for measurements, followed by Tukey's post-hoc test to compare procedures.

**Acknowledgements:** This work was supported by the National Research Foundation of Korea funded by the Ministry of Education, Science and Technology (MEST) (No. 2009-0081467, 2008-0062413, 2010-0026575), by a Korea Student Aid Foundation (KOSAF) grant funded by the MEST (No. S2-2009-000-00972-1), and by the Korea Science & Engineering Foundation through the Infection Signaling Network Research Center (R13-2007-020-01000-0) at Chungnam National University.

**Conflict of interest:** The authors declare no financial or commercial conflict of interest.

### References

- 1 Taoka, Y., Okajima, K., Uchiba, M., Murakami, K., Kushimoto, S., Johno, M., Naruo, M. et al., Role of neutrophils in spinal cord injury in the rat. *Neuroscience* 1997. 79: 1177–1182.
- 2 Popovich, P. G., Wei, P. and Stokes, B. T., Cellular inflammatory response after spinal cord injury in Sprague-Dawley and Lewis rats. *J. Comp. Neurol.* 1997. 377: 443–464.
- 3 Bareyre, F. M. and Schwab, M. E., Inflammation, degeneration and regeneration in the injured spinal cord: insights from DNA microarrays. *Trends Neurosci.* 2003. 26: 555–563.
- 4 Hamada, Y., Ikata, T., Katoh, S., Nakauchi, K., Niwa, M., Kawai, Y. and Fukuzawa, K., Involvement of an intercellular adhesion molecule 1-dependent pathway in the pathogenesis of secondary changes after spinal cord injury in rats. *J. Neurochem.* 1996. 66: 1525–1531.
- 5 Popovich, P. G., Guan, Z., Wei, P., Huitinga, I., van Rooijen, N. and Stokes, B. T., Depletion of hematogenous macrophages promotes partial hindlimb recovery and neuroanatomical repair after experimental spinal cord injury. *Exp. Neurol.* 1999. 158: 351–365.
- 6 Liu, Y., Tachibana, T., Dai, Y., Kondo, E., Fukuoka, T., Yamanaka, H. and Noguchi, K., Heme oxygenase-1 expression after spinal cord injury: the induction in activated neutrophils. *J. Neurotrauma* 2002. 19: 479–490.
- 7 Bouhy, D., Malgrange, B., Multon, S., Poirrier, A. L., Scholtes, F., Schoenen, J. and Franzen, R., Delayed GM-CSF treatment stimulates axonal regeneration and functional recovery in paraplegic rats via an increased BDNF expression by endogenous macrophages. *FASEB. J.* 2006. 20: 1239–1241.
- 8 Imai, M., Watanabe, M., Suyama, K., Osada, T., Sakai, D., Kawada, H., Matsumae, M. et al., Delayed accumulation of activated macrophages and inhibition of remyelination after spinal cord injury in an adult rodent model. *J. Neurosurg. Spine* 2008. 8: 58–66.
- 9 Stirling, D. P., Liu, S., Kubes, P. and Yong, V. W., Depletion of Ly6G/Gr-1 leukocytes after spinal cord injury in mice alters wound healing and worsens neurological outcome. *J. Neurosci.* 2009. 29: 753–764.
- 10 Bomstein, Y., Marder, J. B., Vitner, K., Smirnov, I., Lisaey, G., Butovsky, O., Fulga, V. et al., Features of skin-coincubated macrophages that promote recovery from spinal cord injury. *J. Neuroimmunol.* 2003. 142: 10–16.
- 11 Greten, F. R., Eckmann, L., Greten, T. F., Park, J. M., Li, Z. W., Egan, L. J., Kagnoff, M. F. et al., IKKbeta links inflammation and tumorigenesis in a mouse model of colitis-associated cancer. *Cell* 2004. 118: 285–296.
- 12 Rothwarf, D. M. and Karin, M., The NF-kappa B activation pathway: a paradigm in information transfer from membrane to nucleus. *Sci. STKE* 1999. 1999: RE1.
- 13 Barnes, P. J. and Karin, M., Nuclear factor-kappaB: a pivotal transcription factor in chronic inflammatory diseases. *N. Engl. J. Med.* 1997. 336: 1066–1071.
- 14 Dong, H., Fazzaro, A., Xiang, C., Korsmeyer, S. J., Jacquin, M. F. and McDonald, J. W., Enhanced oligodendrocyte survival after spinal cord injury in Bax-deficient mice and mice with delayed Wallerian degeneration. *J. Neurosci.* 2003. 23: 8682–8691.
- 15 Greter, M., Heppner, F. L., Lemos, M. P., Odermatt, B. M., Goebels, N., Laufer, T., Noelle, R. J. et al., Dendritic cells permit immune invasion of the CNS in an animal model of multiple sclerosis. *Nat. Med.* 2005. 11: 328–334.
- 16 Kigerl, K. A., Gensel, J. C., Ankeny, D. P., Alexander, J. K., Donnelly, D. J. and Popovich, P. G., Identification of two distinct macrophage subsets with divergent effects causing either neurotoxicity or regeneration in the injured mouse spinal cord. *J. Neurosci.* 2009. 29: 13435–13444.
- 17 Slatery, M. J., Liang, S. and Dong, C., Distinct role of hydrodynamic shear in leukocyte-facilitated tumor cell extravasation. *Am. J. Physiol. Cell Physiol.* 2005. 288: C831–C839.
- 18 Kobayashi, Y., The role of chemokines in neutrophil biology. *Front Biosci.* 2008. 13: 2400–2407.
- 19 Basso, D. M., Fisher, L. C., Anderson, A. J., Jakeman, L. B., McTigue, D. M. and Popovich, P. G., Basso Mouse Scale for locomotion detects differences in recovery after spinal cord injury in five common mouse strains. *J. Neurotrauma* 2006. 23: 635–659.
- 20 Zemans, R. L. and Arndt, P. G., Tec kinases regulate actin assembly and cytokine expression in LPS-stimulated human neutrophils via JNK activation. *Cell Immunol.* 2009. 258: 90–97.
- 21 Bao, F., Bailey, C. S., Gurr, K. R., Bailey, S. I., Rosas-Arellano, M. P., Dekaban, G. A. and Weaver, L. C., Increased oxidative activity in human blood neutrophils and monocytes after spinal cord injury. *Exp. Neurol.* 2009. 215: 308–316.
- 22 Im, J. Y., Kim, D., Paik, S. G. and Han, P. L., Cyclooxygenase-2-dependent neuronal death proceeds via superoxide anion generation. *Free Radic. Biol. Med.* 2006. 41: 960–972.
- 23 Zhu, C., Wang, X., Qiu, L., Peeters-Scholte, C., Hagberg, H. and Blomgren, K., Nitrosylation precedes caspase-3 activation and translocation of

- apoptosis-inducing factor in neonatal rat cerebral hypoxia-ischaemia. *J. Neurochem.* 2004. **90**: 462–471.
- 24 Gu, Z., Kaul, M., Yan, B., Kridel, S. J., Cui, J., Strongin, A., Smith, J. W. et al., S-nitrosylation of matrix metalloproteinases: signaling pathway to neuronal cell death. *Science* 2002. **297**: 1186–1190.
- 25 Wu, K. L., Chan, S. H., Chao, Y. M. and Chan, J. Y., Expression of pro-inflammatory cytokine and caspase genes promotes neuronal apoptosis in pontine reticular formation after spinal cord transection. *Neurobiol. Dis.* 2003. **14**: 19–31.
- 26 Takadera, T., Yumoto, H., Tozuka, Y. and Ohyashiki, T., Prostaglandin E(2) induces caspase-dependent apoptosis in rat cortical cells. *Neurosci. Lett.* 2002. **317**: 61–64.
- 27 Yu, F., Kamada, H., Niizuma, K., Endo, H. and Chan, P. H., Induction of mmp-9 expression and endothelial injury by oxidative stress after spinal cord injury. *J. Neurotrauma* 2008. **25**: 184–195.
- 28 Clausen, B. E., Burkhardt, C., Reith, W., Renkawitz, R. and Forster, I., Conditional gene targeting in macrophages and granulocytes using LysMcre mice. *Transgenic Res.* 1999. **8**: 265–277.
- 29 Li, Z. W., Omori, S. A., Labuda, T., Karin, M. and Rickert, R. C., IKK beta is required for peripheral B cell survival and proliferation. *J. Immunol.* 2003. **170**: 4630–4637.
- 30 Hong, J., Cho, I. H., Kwak, K. I., Suh, E. C., Seo, J., Min, H. J., Choi, S. Y. et al., Microglial toll-like receptor 2 contributes to kainic acid-induced glial activation and hippocampal neuronal cell death. *J Biol Chem* 2010. **285**: 39447–39457.
- 31 Brechtel, K., Tura, A., Abdibzadeh, M., Hirsch, S., Conrad, S. and Schwab, J. M., Intrinsic locomotor outcome in dorsal transection of rat spinal cord: predictive value of minimal incision depth. *Spinal Cord* 2006. **44**: 605–613.
- 32 Michel, R.P. and Cruz-Orive, L.M., Application of the Cavalieri principle and vertical sections method to lung: estimation of volume and pleural surface area. *J. Microsc.* 1988. **150**: 117–136.
- 33 Lee, H., Jo, E. K., Choi, S. Y., Oh, S. B., Park, K., Kim, J. S. and Lee, S. J., Necrotic neuronal cells induce inflammatory Schwann cell activation via TLR2 and TLR3: implication in Wallerian degeneration. *Biochem. Biophys. Res. Commun.* 2006. **350**: 742–747.
- 34 Livak, K. J. and Schmittgen, T. D., Analysis of relative gene expression data using real-time quantitative PCR and the 2<sup>-Delta Delta C(T)</sup> Method. *Methods* 2001. **25**: 402–408.
- 35 de Almeida, M. C., Silva, A. C., Barral, A. and Barral Netto, M., A simple method for human peripheral blood monocyte isolation. *Mem. Inst. Oswaldo Cruz.* 2000. **95**: 221–223.
- 36 Yamamoto, S., Shimizu, S., Kiyonaka, S., Takahashi, N., Wajima, T., Hara, Y., Negoro, T. et al., TRPM2-mediated Ca<sup>2+</sup> influx induces chemokine production in monocytes that aggravates inflammatory neutrophil infiltration. *Nat. Med.* 2008. **14**: 738–747.
- 37 Frederiks, W. M. and Mook, O. R., Metabolic mapping of proteinase activity with emphasis on in situ zymography of gelatinases: review and protocols. *J. Histochem. Cytochem.* 2004. **52**: 711–722.

**Abbreviations:** 8-OHG: 8-hydroxy-guanine · BMS: Basso Mouse Scale · CXCL: CXC ligand · dpi: days post-injury · IKK: IκB kinase · MMP-9: matrix metalloproteinase 9 · SCI: spinal cord injury

**Full correspondence:** Dr. Sung Joong Lee, Department of Neuroscience, School of Dentistry, Seoul National University, 28 Yeongun-dong, Jongro-gu, Seoul 110-749, South Korea  
Fax: +82-2-762-5107  
e-mail: sjlee87@snu.ac.kr

Received: 15/4/2010  
Revised: 19/12/2010  
Accepted: 10/2/2011  
Accepted article online: 10/3/2011